TECHNISCHE MECHANIK, Band 28, Heft 1, (2008), 3 – 12
Manuskripteingang: 31. August 2007

Experimental and Numerical Investigation of Size Effects in Polyurethane Adhesive Sealings

M. Johlitz, H. Steeb, S. Diebels, J. Batal, W. Possart

In our contribution we present an extended continuum-based material model which is able to capture size effects in adhesive bonds. The model is based on the introduction of a scalar-valued structure parameter and its related postulated balance equation. On the experimental side we perform shear tests on polyurethane bonds of anodised aluminium by using different shear rates and different thicknesses of the bonded joints. The results of these shear tests show a thickness-dependent stiffness behaviour of the specimens. Finally the obtained experimental data are fitted with the extended material model. The introduced model parameters are identified by using an optimisation tool based on biologic evolution strategies.

1 Introduction

Adhesives are able to produce boundary layers when they contact substrates (Sanctuary et al., 2003; Krüger et al., 2004; Bouchet et al., 2002; Bouchet and Roche, 2002; Fata, 2005). There are different physical reasons for these boundary layers which are not yet understood in detail. However they can have a significant influence on the effective mechanical behaviour of the joints which, in our case, is reflected in the form of a size effect *thinner is weaker* as observed by several shear experiments, cf. Diebels et al. (2007). These experiments were performed by using anodised aluminium substrates which were glued together with a polyurethane (PUR) composed of three monomers from the Bayer AG. Different bonding thicknesses from $78\,\mu\mathrm{m}$ up to $2270\,\mu\mathrm{m}$ were investigated. Although this polyurethane elastomer shows a typical rate-dependent viscoelastic material behaviour, we restrict discussion to the basic elasticity in this contribution. The rate dependent behaviour of the adhesive layers will be investigated separately in an upcoming paper. Recapitulating, one can say that the macroscopic stiffness of bonds may depend on their thickness, on the substrate and on the surface treatment thereof. This renders the traditional description of bonded joints mechanical behaviour with macroscopic bulk material models impossible.
Therefore we have developed an extended phenomenological macroscopic material model which is able to capture the above described phenomena. The model is based on the introduction of a scalar-valued structure parameter κ and its related balance equation. This structure parameter describes local properties without going into detail and without the need of knowing the processes in the microstructure respectively. Conceptually the modelling approach with an additional degree of freedom is based on the work of Capriz (1980), Capriz et al. (1982), Svendsen (1999, 2001), Steeb and Diebels (2004) and Diebels et al. (2005, 2007). Hence the structure parameter describes the observed size effect in an abstract manner and it controls the mechanical stiffness behaviour of the bond. For very thick bonds the bulk value of the used PUR is achieved, for thin bonds the boundary layer is dominating the material behaviour as will be shown in the following investigations. The introduced model parameters are at least identified by solving the inhomogenieous boundary value problem in combination with a parameter identification tool based on biologic evolution strategy methods, cf. Rechenberg (1973) and Schwefel (1995). The paper closes with a conclusion and an outlook.

2 Sample Preparation, Setup and Experimental Results

In this chapter we introduce the sample preparation and the experimental setup of our shear test.
The polymer is a two-part system formed by polyaddition of Bayer Desmodur CD® (89 % diphenylmethane-4,4'-diisocyanate, 11 % urethoneimine triisocyanate additive) with a polyol mixture of Bayer Desmophen 2060 BD® (linear polypropylene ether diol) and Bayer Desmophen 1380 BT® (branched polypropylene ether triol) in the stoichiometric ratio of isocyanate (NCO) and hydroxyl groups, cf. figure 1 for chemical structures in detail.

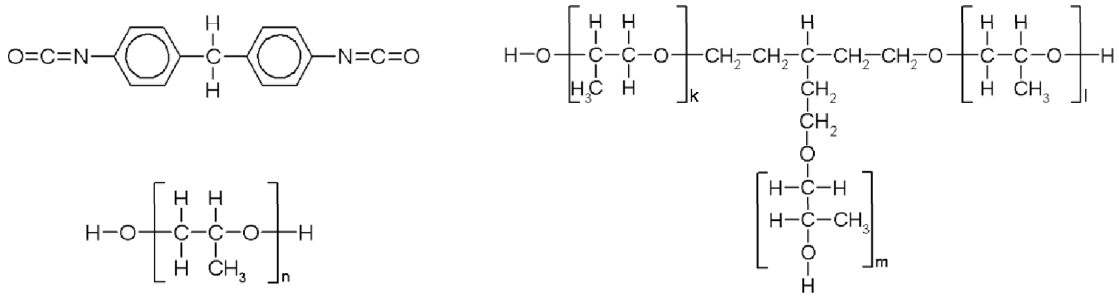

Figure 1: Diphenylmethane-4,4'-diisocyanate (upper left), linear polypropylene ether diol (lower left) and branched polypropylene ether triol (right)

The components are stored and mixed in desiccated air within a glove box to avoid parasitic reactions of the isocyanate groups with water. After thoroughly stirring the components, the batch is vacuum-degassed at 2 torr for 10 minutes. Testing this step with the single components, no significant mass loss was detected. The resulting mixture is homogeneous and free of bubbles.
The chemical reaction of Desmophen 2060 BD® with Desmodur CD® results in linear chains while Desmophen 1380 BT® contributes cross-links because of its trifunctionality. Hence the mechanical behaviour of the polymer glue can be adjusted by the mixing ratio of triol and diol. In this case we set the ratio of functional groups to $\mathrm{OH_{triol}} : \mathrm{OH_{diol}} = 80 : 20$. The resulting material behaviour of the polymer can be described as a typical viscoelastic elastomer at room temperature.

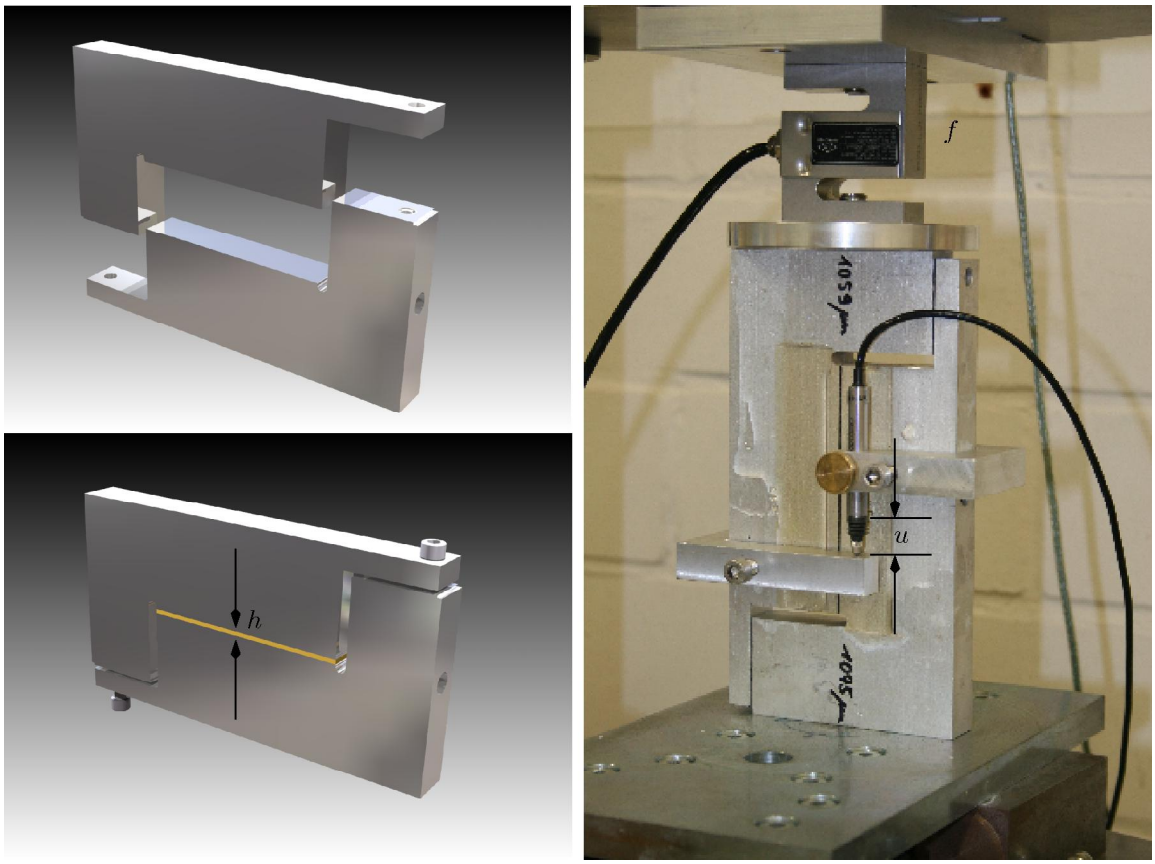

Figure 2: Preparated shear sample (left) and experimental setup of the shear test (right)

For the preparation of PU adhesive joints, aluminium blocks (AlMg3) are spark-eroded into halves (cf. Fig. 2). The resulting surfaces have an excellent fit and are free of burs. The halves are ultrasonically-degreased in acetone, etched (1-molar NaOH, 10 min.), pickled ($20\,\%\ \mathrm{HNO_3}$, 1 min.), rinsed with distilled water and ethanol, and finally vacuum-dried in an oven at 120° C. The samples are then anodised for 2 hours in $5\,\%$ oxalic acid at a current of $0.1\,\mathrm{A/cm^2}$. During anodisation the acid was chilled to approximately 35° C. After further rinsing and vacuumdrying, spacers are positioned between the non-bonded surfaces. The halves are then prefixed with screws.

In this state the width of the gap between the halves was precisely measured with a Quadra-Check microscope. Finally, before bonding, the prepared shear samples were kept in dried air within the glove box for 1 day. Thus, adsorbed water from the surface dried. The joint was then formed with the above PUR mixture, vacuum degassed twice, cross-linked at RT for 72 h and post-cured at 50° C for another hour. 34 specimens were made, having bonding thicknesses between 78 μm and 2270 μm. The maximum deviation in parallelism of the joints was 1.5%. The basis of the experimental investigation is a frame shear machine RS5 from the company GIESA. Since this machine has no sufficient time resolution (only 1 Hz) it was enhanced by a custom made sensor system. Figure 2 (right) shows the experimental setup with all components. A force sensor with a range of 10 kN at a resolution of 1 N and an inductive displacement sensor with a range of 2 mm at a resolution of 1 μm are fixed in the centerline of the sample. They are able to transfer data with a sampling rate of up to 1 kHz. Consequentely, the effective shear strain γ can be calculated by the ratio of the measured deformation u and the bond thickness h. Furthermore the effective shear stress τ is calculated by the ratio of the measured force f and the area of the adhesive joint A. At first, the relation between constant shear rates and the bond thickness was investigated in order to define and calculate thickness-dependent constant shear rates which do not activate the time dependency of the material. Figure 3 shows a part of the obtained results for illustration. In the left graph one can see the experimental data of the stress-strain behaviour of the PUR under isothermal and quasi-static conditions. The right graph shows the calculated slope of all obtained stress-strain lines which is defined as the effective shear modulus μ_{eff}. These effective moduli $\mu_{eff} := \partial\tau/\partial\gamma|_{\gamma=0}$ are plotted versus the bond thickness h. Both pictures perform a significant size effect in the form *thinner is weaker*. To simplify matters the received relation between the effective modulus and the bonding thickness was fitted mathematically via a nonlinear regression as seen in figure 3, right (solid line). This approach will be helpful in the parameter identification procedure as will be demonstrated later.

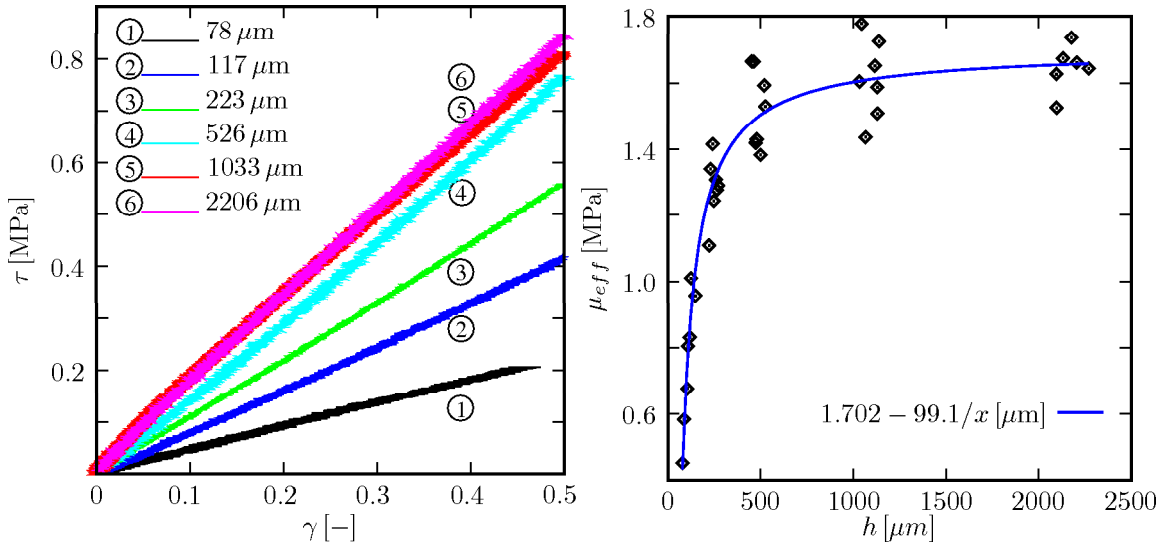

Figure 3: Experimental results: Stress-stain behaviour of different samples for the basic elasticity (left) and effective shear modulus versus bonding thickness (right)

As a main result from the experimental investigation we find a strong size effect in the form *thinner is weaker*, i.e. the effective stiffness is a function of the layer thickness. Bulk properties are obtained only if the layers are 2 mm or thicker.

3 Modelling Aspects

In this chapter we present a phenomenological continuum mechanical model which is able to describe the above mentioned size effects.
The starting point are the experimental results and characteristics of the bulk material. From quasi-static tests the bulk behaviour is characterized to be hyperelastic. The model parameters are obtained from uniaxial tension tests and from shear tests performed on specimens with a thick poylurethane layer ($h \geq 2000\,\mu$m) to diminish the influence of boundary layers near the substrates in relation to the stiffness of the complete bond. In this case, the parameters can be identified by using a commercial fitting tool with respect to the analytical solution of the homogeneous boundary value problem. Afterwards we focus on the experimental results of the shear tests which show a significant strong size effect in the form *smaller is weaker*. It becomes evident that a classical continuum mechanical theory is not able to model this effect. Extended continuum theories in the meaning of Eringen (1999)

also only allow to model size effects in the form *smaller is stiffer*. Our experimental results require the modelling of a weakening effect so that we present an exended continuum mechanical model based on the introduction of a dimensionless scalar-valued structure parameter $\kappa(\mathbf{x}, t)$ and its postulated balance equation. This structure parameter abstractly summarises the effect of the local processes taking place close to the surface of the substrates. The advantage of such a phenomenological approach is the fact that it does not require a detailed knowledge of the physical and chemical processes governing the formation of the boundary layer. Furthermore this approach is able to model both forms of size effects depending on the choice of the boundary condition of the structure parameter. The model has two primary variables, the vector-valued displacement field $\mathbf{u}(\mathbf{x}, t)$ and the scalar-valued structure parameter $\kappa(\mathbf{x}, t)$. For each quantity a balance equation is postulated. This yields the balance of momentum

$$\operatorname{div} \mathbf{T} = \mathbf{0} \tag{1}$$

and an additional balance for the structure parameter κ

$$\operatorname{div} \mathbf{S} + \hat{\kappa} = 0. \tag{2}$$

In this connection we restrict ourselves to the quasi-static case under isothermal conditions without considering long-range effects for both quantities. The symbols introduced in (1) and (2) are the Cauchy stress tensor $\mathbf{T}$, the vector-valued flux $\mathbf{S}$ related to κ and a production term $\hat{\kappa}$. Note that equation (2) possesses the same structure as the *balance of equilibrated forces* introduced by Goodman and Cowin (1972).
There are different possibilities to motivate the above described additional balance. Another approach is starting with an extended balance of energy so that the additional balance (2) is derived from invariance requirements, cf. Capriz (1980); Capriz et al. (1982); Svendsen (2001) or from thermodynamical considerations, cf. Steeb and Diebels (2004). Here we strictly follow the approach of the postulate.
Following the usual arguments the balance of energy is split into a mechanical part and the balance of internal energy.

$$\rho \dot{\varepsilon} = \mathbf{T} : \mathbf{D} + \mathbf{S} \cdot \operatorname{grad} \dot{\kappa} - \hat{\kappa} \dot{\kappa} \,. \tag{3}$$

Herein $\rho \dot{\varepsilon}$ stands for the time derivative of the internal energy density and $\mathbf{T} : \mathbf{D}$ is the stress power. A dot represents a single contraction between the basis vectors of the tensor bases whereas a colon means a double contraction. The coupling of the balance of internal energy with the balance of entropy including the Legendre transformation yields the extended Clausius-Planck inequality

$$-\rho \dot{\Psi} + \mathbf{T} : \mathbf{D} + \mathbf{S} \cdot \operatorname{grad} \dot{\kappa} - \hat{\kappa} \dot{\kappa} \geq 0 \,. \tag{4}$$

In this inequality the term $\rho \dot{\Psi}$ expresses the time derivative of the free Helmholtz energy density with Ψ as the specific free Helmholtz energy. Before evaluating the entropy principle it is necessary to choose a set of process variables. This is done for the simplest way in the form

$$\mathcal{S} = \{\mathbf{B},\, \kappa,\, \operatorname{grad} \kappa\}. \tag{5}$$

In (5) $\mathbf{B}$ is the left Cauchy-Green deformation tensor calculated from the deformation gradient $\mathbf{F}$ according to

$$\mathbf{B} = \mathbf{F} \cdot \mathbf{F}^T, \qquad \mathbf{F} = \mathbf{I} + \operatorname{Grad} \mathbf{u}. \tag{6}$$

Here the identity tensor $\mathbf{I}$ is introduced and the gradient operator $\operatorname{Grad}(\bullet)$ is a measurement with respect to the position vector $\mathbf{X}$ of the reference configuration whereas $\operatorname{grad}(\bullet)$ is the gradient operator with respect to the position vector $\mathbf{x}$ of the current configuration. The displacement field $\mathbf{u} = \mathbf{x} - \mathbf{X}$ is computed by the difference of the two position vectors. The symbol $(\bullet)^T$ refers to the transposed tensor.
The evaluation of the entropy principle corresponding to the classical argumentation of Coleman and Noll (1963)

is leading to the following set of constitutive equations which can be computed from the partial derivations of the specific free Helmholtz energy function Ψ to

$$\mathbf{T} = 2\,\rho\,\mathbf{B}\cdot\frac{\partial\Psi}{\partial\mathbf{B}}\;, \qquad \mathbf{S} = \rho\frac{\partial\Psi}{\partial\mathrm{grad}\kappa}\;, \qquad -\hat{\kappa} = \rho\frac{\partial\Psi}{\partial\kappa}\;. \tag{7}$$

In order to include the experimentally observed size effect it is necessary to choose an adequate free energy function Ψ. For numerical reasons, but without constraining the developed theory, we apply a volumetric-isochoric split of the free energy function Ψ, cf. Flory (1961). Due to the fact that our investigated polyurethane is almost incompressible this approach does not cause unphysical results as demonstrated in the work of Ehlers and Eipper (1999) for compressible materials.
The starting point is the multiplicative decomposition of the deformation gradient $\mathbf{F}$ into a volumetric and an isochoric part, cf. Flory (1961), according to

$$\mathbf{F} = J^{\frac{1}{3}}\,\bar{\mathbf{F}} \;\Leftrightarrow\; \bar{\mathbf{F}} = J^{-\frac{1}{3}}\,\mathbf{F}\,, \tag{8}$$

whereas $\det\bar{\mathbf{F}} = 1$ and $J = \det\mathbf{F} = \sqrt{\det\mathbf{B}}$ stands for the Jacobian. Hence the complete volumetric deformation is described by the term $J^{\frac{1}{3}}$. The computation of the isochoric left Cauchy-Green tensor $\bar{\mathbf{B}}$ and its related isochoric first invariant $\bar{\mathrm{I}}_{\mathbf{B}}$ results in

$$\bar{\mathbf{B}} = J^{-\frac{2}{3}}\,\mathbf{B} \qquad \bar{\mathrm{I}}_{\mathbf{B}} = J^{-\frac{2}{3}}\,\mathrm{I}_{\mathbf{B}}\,. \tag{9}$$

The free Helmholtz energy density has to be chosen according to the experimental results. For simplicity we opted for an additiv decomposition, cf. Diebels et al. (2007).

$$\rho_0\,\Psi \;=\; \Psi_{iso}(\bar{\mathrm{I}}_{\mathbf{B}}) \;+\; \Psi_{vol}(J) \;+\; \Psi_{struct}(\kappa,\,\mathrm{grad}\;\kappa) \;+\; \Psi_{couple}(\kappa,\,\bar{\mathrm{I}}_{\mathbf{B}}). \tag{10}$$

The first term on the right side of equation (10) represents the standard free energy density term of the incompressible Neo-Hooke material

$$\Psi_{iso} \;=\; \tfrac{1}{2}\,\mu\,\left(\bar{\mathrm{I}}_{\mathbf{B}} \;-\; 3\right), \tag{11}$$

while

$$\Psi_{vol} \;=\; \tfrac{1}{4}\,K\,\left((J\;-\;1)^2 \;+\; (\ln J)^2\right) \tag{12}$$

is a polyconvex volumetrical extension term formulated in the Jacobian J. In this context we introduce the bulk modulus K and the shear modulus μ as material parameters describing the mechanical bulk behaviour of the polyurethane. For quasi-incompressible materials K has to be much larger than the shear modulus μ. One can say that it acts like a penalty term.
The mathematical expression concerning the structure parameter κ and its gradient $\mathrm{grad}\,\kappa$ is assumed to be as simple as possible, i.e. a quadratic ansatz is chosen:

$$\Psi_{struct} \;=\; \tfrac{1}{2}\,\alpha\,\kappa^2 \;+\; \tfrac{1}{2}\,\xi\,(\mathrm{grad}\,\kappa)^2. \tag{13}$$

Equation (13) introduces the additional model parameters α and ξ. Furthermore, the most important part of the free Helmholtz energy function is the coupling term which allows to combine the investigated balance equation on a constitutive level. This part is chosen to be

$$\Psi_{couple} = \delta(\phi^{\kappa} - 1)\,\big(\bar{\mathrm{I}}_{\mathbf{B}} - 3\big) \tag{14}$$

introducing further model parameters δ and ϕ. The motivation of this term becomes clear when evaluating (11) – (14) according to (7). This yields the constitutive equations for the Cauchy stress tensor $\mathbf{T}$, the flux vector $\mathbf{S}$ and the scalar production term $\hat{\kappa}$ in the following form

$$\begin{aligned}
\mathbf{T} &= J^{-1}\big(\tfrac{1}{2}\,K\,(J^2 - J + \ln J)\,\mathbf{I} + (\mu + 2\,\delta(\phi^{\kappa} - 1))\,\mathbf{B}_{iso}\big), \\
\mathbf{S} &= J^{-1}\,\xi\,\operatorname{grad}\kappa, \\
\hat{\kappa} &= -\,J^{-1}\big(\alpha\,\kappa + \delta\,\phi^{\kappa}\,\ln\phi(\bar{\mathrm{I}}_{\mathbf{B}} - 3)\big).
\end{aligned} \tag{15}$$

Note that the equations in (15) are formulated with respect to the current configuration. Here we make the restrictions that the term $\mu + 2\,\delta(\phi^{\kappa} - 1)$ has to be greater than 0 not to loose the stiffness of the system and that the parameter ϕ has to be greater than 1. The second order tensor $\mathbf{B}_{iso}$ is the abbreviation for the mathematical expression

$$\mathbf{B}_{iso} = \quad \bar{\mathbf{B}} - \tfrac{1}{3}\,\bar{\mathrm{I}}_{\mathbf{B}}\,\mathbf{I} \;= J^{-\frac{2}{3}}\,\mathbf{B} - \tfrac{1}{3}\,J^{-\frac{2}{3}}\,\mathrm{I}_{\mathbf{B}}\,\mathbf{I}\,. \tag{16}$$

By studying the constitutive equations one can give a first explanation of the functionality of the structure parameter κ and its related equations. As can be seen κ is coupling inside the macroscopic material law. This means in detail that κ specifically influences the macroscopic deformation measure. Once the structure parameter equals 0 there is no influence and bulk behaviour is obtained. For $\kappa \geq 0$ and $\kappa \leq 0$ we get decreased and increased stiffness, respectively.

4 Numerical Realisation and Parameter Identification

In this section we briefly describe the numerical implementation of the extended material model. For details concerning the numerical implementation into a coupled Finite Element framework we refer to the work of Steeb and Diebels (2004).
The balance equations (1), (2) as well as the constitutive equations (15) lead to a set of coupled differential equations for the displacement field $\mathbf{u}$ and for the structure parameter κ. Both Dirichlet and Neumann boundary conditions can be prescribed on the boundary Γ for the variables $\mathbf{u}$ and κ. The specification of the boundary values entails the following standard mathematical expressions

$$\left.\begin{aligned}
\mathbf{u} &= \bar{\mathbf{u}} \;\text{ on }\; \Gamma_D^{\mathbf{u}} \quad\text{and}\quad \mathbf{t} = \bar{\mathbf{t}} \;\text{ on }\; \Gamma_N^{\mathbf{u}} \\
\kappa &= \bar{\kappa} \;\text{ on }\; \Gamma_D^{\kappa} \quad\text{and}\quad s = \bar{s} \;\text{ on }\; \Gamma_N^{\kappa}
\end{aligned}\right\}, \tag{17}$$

with

$$\Gamma_D^{\mathbf{u}} \cup \Gamma_N^{\mathbf{u}} = \Gamma_D^{\kappa} \cup \Gamma_N^{\kappa} = \partial B \quad \text{with} \quad \Gamma_{\mathrm{D}}^{\mathbf{u}} \cap \Gamma_{\mathrm{N}}^{\mathbf{u}} = \emptyset \quad \text{and} \quad \Gamma_{\mathrm{D}}^{\kappa} \cap \Gamma_{\mathrm{N}}^{\kappa} = \emptyset \tag{18}$$

Starting with the balance equations (1), (2) the weak form results from mathematical considerations for the balance of momentum in

$$\int_B \mathbf{T} : \operatorname{grad}\delta\mathbf{u}\,\mathrm{dv} = \int_{\partial B} \bar{\mathbf{t}} \cdot \delta\mathbf{u}\,\mathrm{da}\,, \tag{19}$$

and for the additional balance of the structure parameter in

$$\int_B \mathbf{S} \cdot \operatorname{grad} \delta\kappa \, \mathrm{dv} = \int_{\partial B} \bar{s} \, \delta\kappa \, \mathrm{da} + \int_B \hat{\kappa} \, \delta\kappa \, \mathrm{dv} \,, \tag{20}$$

with the test functions $\delta\mathbf{u}$ and $\delta\kappa$ respectively. These weak forms were implemented in the finite element solver PANDAS, Ehlers and Ellsiepen (1998), while solving them numerically with a coupled multifield Galerkin finite element method, Steeb and Diebels (2004), in combination with the constitutive relations (15).
In the present case, we prescribe the usual Dirichlet and Neumann data for the displacement field $\mathbf{u}$ according to the corresponding shear experiments. For the field of the structure parameter κ we prescribe only Dirichlet boundary conditions in the form $\bar{\kappa} = 1$ or $\bar{\kappa} = -1$ subject to stiffening or weakening size effects which are observed in the experimental investigations. Here we choose $\bar{\kappa} = -1$ at the boundaries close to the substrates meeting the observed weakening effect. Therefore, the dimensionless value $\bar{\kappa}$ characterises the properties of the adhesive bond between the polymer and the substrate and its influence with respect to the boundary layer. The assumption of the values of the Dirichlet boundary conditions of the scalar structure parameter is arbitrary. Therefore $\bar{\kappa} = -1$ characterises PUR on anodised aluminium. We intend to use modified values for the boundary conditions of the structure parameter when using substrates or other treated surfaces. Note again, that the phenomenological approach does not require a detailed explanation of the physical and chemical processes taking place in the boundary layer near the substrates.
Finally the presented model has to be adapted to the experimental data given by the performed tests (cf. figure 3). Data were obtained in uniaxial tension tests and in shear tests.
The strategy of the identification is a two-step procedure: First, the bulk parameters μ and $K \gg \mu$ are determined from tension tests and from shear tests for very thick adhesive sealings.
Second, the additional model parameters α, ξ, δ and ϕ are determined by using the data which we obtained from the shear tests in the form of a size effect. The procedural method will be explained after a short introduction into the used parameter identification tool.
In this paper we use a flexible tool for the identification based on a genetic algorithm, cf. Schwefel (1995). Starting point of the procedure is the generation of N sets of parameters $\mathcal{P}_i = \{\alpha_i, \, \xi_i, \, \delta_i \, \phi_i\}$ which are chosen arbitrarily. These parameter sets are the so-called parents. For each of the parents the model is evaluated according to the boundary value problem which corresponds to the performed experiment. An objective function Q is defined as the sum of the squares of differences between measured data f_{exp} and computed data f_{model}, that is

$$Q = \sum_i (f_{exp} - f_{model}(\mathcal{P}_i))^2. \tag{21}$$

Our goal is to minimise the objective function Q with respect to the model parameters $\mathcal{P}$. Therefore, a certain number M of the N parents is chosen leading to the smallest values of Q. From these parents a new generation is generated which is called children. The children are generated according to principles of evolution, i. e. parameters of different parents are re-combined, some of the parameters are slightly changed, some are chosen arbitrarily by a random number generation. If N children are generated these children form the next generation and the algorithm starts again. The procedure is continued until the objective function reaches its global minimum.

In our case, the parameter were identified as follows:

First of all we identified the shear modulus $\mu = 1.70\,\mathrm{MPa}$ by using the data of the performed uniaxial tension tests in combination with the analytical solution of this test. We took into account incompressible material behaviour and a commercial fitting tool. Accordingly we made a numerical study of the influence of the bulk modulus $K \gg \mu$ and found that $K = 500\,\mathrm{MPa}$ is the value which is able to describe a nearly incompressible material behaviour.
We verified these values by further investigations with our identification tool based on evolution strategies. Therefore we set $\kappa = 0$ for the whole domain and $\bar{\kappa} = 0$ at the boundaries. This means that no boundary layer is present which would be able to produce a size effect.
Then we generated six boundary value problems with the bonding thickness of $100\,\mu\mathrm{m}$, $200\,\mu\mathrm{m}$, $300\,\mu\mathrm{m}$, $500\,\mu\mathrm{m}$, $1000\,\mu\mathrm{m}$ and $2000\,\mu\mathrm{m}$, respectively, close to the real shear experiments. The optimisation function was formulated in the effective shear modulus μ_{eff}. Therefore we calculated the experimental values according to figure 3, right.
Accordingly the above described procedure was started. It turned out that the model parameter ξ is not sensitive with respect to the solution of the balance of momentum and that the additional balance of the structure parameter is only controlled by the ratio of the parameter α to the parameter ξ. For this reasons the parameter ξ was fixed and set to $\xi = 1\,\mathrm{MPa}$.
Following, the procedure was started again and the optimum output of the remaining model parameters α, δ

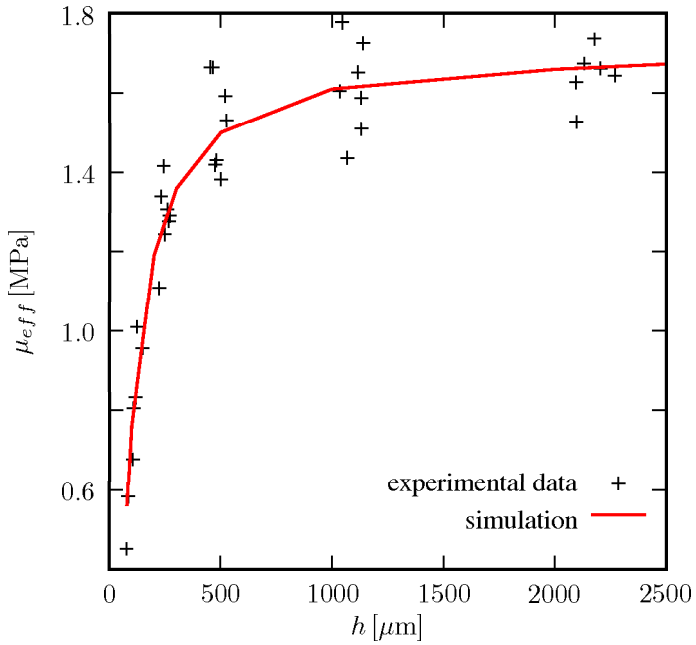

Figure 4: Effective shear modulus μ_{eff} [MPa] versus bonding thickness h [μm], comparison of the experimental data and numerical simulation.

and ϕ was found after 70-100 generations. The values were found to be $\alpha = 35000\,\mathrm{MPa}$, $\delta = 1.82\,\mathrm{MPa}$ and $\phi = 1.89\,[-]$.
Hence, we simulated the shear experiments with the extended model including the identified paramters and compared it to the experimental results. Figure 4 shows the effective shear moduli μ_{eff} versus the corresponding bonding thickness for the experiments and for the simulations. One can say that the model excellently describes the observed size effect. The extrapolations of the simulations to a bonding thickness of $2500\,\mu\mathrm{m}$ and $80\,\mu\mathrm{m}$, respectively, also shows an adequate agreement with the experimental data.

5 Conclusion and Outlook

It is well-known from literature that the modelling of adhesive bonds is very difficult with respect to the thickness-dependent stiffness behaviour of such a joint depending on the used polymer (glue) and the substrates. The influence of the surface treatment of the joining partners also significantly influences the mechanical behaviour of a sealing.
In the present contribution we investigated a polyurethane system with commercial components from the Bayer AG which was applied to anodised aluminium substrates. We prepared adhesive joints with a bonding thickness from $78\,\mu\mathrm{m}$ to $2270\,\mu\mathrm{m}$. With these specimens shear tests up to finite deformation were performed. The experimental results show a strong size effect in the form *thinner is weaker*. To express this observed phenomenon in material parameters means that the effective shear modulus of a polymer film between two substrates decreases with the thickness of the bond.
In order to model this experimentally observed effect we developed a phenomenological approach via a scalar-valued structure parameter κ and its related balance which is able to describe local microstructural effects in an abstract manner. The extended continuum mechanical material model allows to map stiffening and weakening effects due to the choice of the boundary condition of the structure parameter.
The parameters of the model were identified by a tool which is based on biologic evolution strategies. This program was used in combination with a nonlinear finite element analysis. Finally, this combination was appropriate to identify the model parameters as shown in numerical simulations.
Future work will focus on the viscoelastic material behaviour of the bonded joints in conjunction with the size effect. Experiments have already shown that this size effect is not only governing the basic elasticity part of the investigated polyurethane. In fact, first experiments have attested that the time-dependent viscoelastic material behaviour is also thickness-dependent.

Acknowledgement

The authors acknowledge the financial support by the German Science Foundation DFG under the grants Di 430/5-1 and Po 577/17-1.

References

Bouchet, J.; Roche, A. A.: The formation of epoxy/metal interphases: Mechanisms and their role in practical adhesion. *J. Adhesion*, 78, (2002), 799–830.

Bouchet, J.; Roche, A. A.; Jacquelin, E.: How do residual stresses and interphase mechanical properties affect practical adhesion of epoxy diamine/metallic substrate system. *J. Adhesion Sci. Technol.*, 12, (2002), 1603–1623.

Capriz, G.: *Continua with Microstructures*. Springer (1980).

Capriz, G.; Podio-Guidugli, P.; Williams, W.: On balance equations for materials with affine structure. *Meccanica*, 17, (1982), 80–84.

Coleman, B. D.; Noll, W.: The thermodynamics of elastic materials with heat conduction and viscosity. *Arch. Rational Mech. An.*, 13, (1963), 167–178.

Diebels, S.; Johlitz, M.; Steeb, H.; Possart, W.; Batal, J.: A macroscopic model of the interphase in thin polymer films based on an order parameter approach. *J. Phys.: Conf. Ser.*, 62, (2007), 34–42.

Diebels, S.; Steeb, H.; Possart, W.: Effects of the interphase on the mechanical behaviour of thin adhesive films – a modeling approach. In: W. Possart, ed., *Adhesion – Current Research and Applications*, John Wiley & Sons (2005).

Ehlers, W.; Eipper, G.: Finite elastic deformations in liquid-saturated and empty porous solids. *Transport Porous Med.*, 34, (1999), 179–191.

Ehlers, W.; Ellsiepen, P.: PANDAS: Ein FE-System zur Simulation von Sonderproblemen der Bodenmechanik. In: P. Wriggers; U. Meißner; E. Stein; W. Wunderlich, eds., *Finite Elemente in der Baupraxis: Modellierung, Berechnung und Konstruktion,* Beiträge *zur Tagung FEM '98 an der TU Darmstadt am 5. und 6. März 1998*, Ernst & Sohn (1998).

Eringen, C.: *Microcontinuum Field Theories, Vol. I: Foundations and Solids*. Springer-Verlag (1999).

Fata, D.: *Epoxidsysteme im Verbund mit rostfreien Stählen – Vernetzung und Alterung*. Universität des Saarlandes (2005).

Flory, P. J.: Thermodynamic relations for hight elastic materials. *Thin Solid Films*, 57, (1961), 829–838.

Goodman, M. A.; Cowin, S. C.: A continuum theory for granular materials. *Arch. Rat. Mech. Anal.*, 44, (1972), 249–266.

Krüger, J. K.; Possart, W.; Bactavachalou, R.; Müller, U.; Britz, T.; Santuary, R.; Alnot, P.: Gradient of the mechanical modulus in glass–epoxy–metal joints as measured by Brillouin microscopy. *J. Adhesion*, 80, (2004), 585–599.

Rechenberg, I.: *Evolutionsstrategie: Optimierung technischer Systeme nach Prinzipien der biologischen Evolution* (1973).

Sanctuary, R.; Bactavatchalou, R.; Müller, U.; Possart, W.; Alnot, P.; Krüger, J. K.: Acoustic profilometry within polymers as performed by Brillouin microscopy. *J. Physics D: Appl. Phys.*, 36, (2003), 2738–2742.

Schwefel, H. P.: *Evolution and Optimum Seeking*. John Wiley & Sons (1995).

Steeb, H.; Diebels, S.: Modeling thin films applying an extended continuum theory based on a scalar-valued order parameter – part I: Isothermal case. *Int. J. Solids Structures*, 41, (2004), 5071–5085.

Svendsen, B.: On the thermodynamics of thermoelastic materials with additional scalar degrees of freedom. *Continuum Mech. Therm.*, 4, (1999), 247–262.

Svendsen, B.: On the continuum modeling of materials with kinematic structure. *Acta Mech.*, 152, (2001), 49–80.

Addresses: Prof. Dr.-Ing. Stefan Diebels, Lehrstuhl für Technische Mechanik, Universität des Saarlandes und Prof. Dr. -rer. nat. habil. Wulff Possart, Lehrstuhl für Adhäsion und Interphasen in Polymeren, Universität des Saarlandes, D-66041 Saarbrücken.
email: `s.diebels@mx.uni-saarland.de`